JACS
JOURNAL OF THE AMERICAN CHEMICAL SOCIETY

ARTICLE

pubs.acs.org/JACS

Nucleophilic Aryl Fluorination and Aryl Halide Exchange Mediated by a Cu^{I}/Cu^{III} Catalytic Cycle

Alicia Casitas,[†] Mercè Canta,[†] Miquel Solà,[†,‡] Miquel Costas,[†] and Xavi Ribas*[,†]

[†]QBIS Research Group, Departament de Química, Universitat de Girona, Campus Montilivi, Girona E-17071, Catalonia, Spain
[‡]Institut de Química Computacional, Universitat de Girona, Campus Montilivi, Girona, E-17071, Catalonia, Spain

Supporting Information

ABSTRACT: Copper-catalyzed halide exchange reactions under very mild reaction conditions are described for the first time using a family of model aryl halide substrates. All combinations of halide exchange (I, Br, Cl, F) are observed using catalytic amounts of Cu^{I}. Strikingly, quantitative fluorination of aryl−X substrates is also achieved catalytically at room temperature, using common F^{-} sources, via the intermediacy of aryl−Cu^{III}−X species. Experimental and computational data support a redox Cu^{I}/Cu^{III} catalytic cycle involving aryl−X oxidative addition at the Cu^{I} center, followed by halide exchange and reductive elimination steps. Additionally, defluorination of the aryl−F model system can be also achieved with Cu^{I} at room temperature operating under a Cu^{I}/Cu^{III} redox pair.

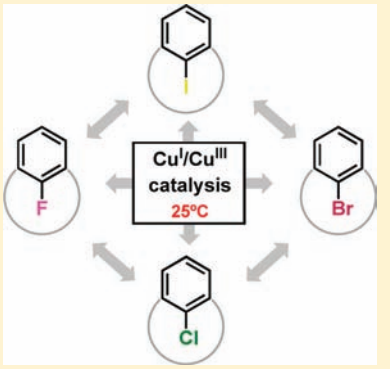

INTRODUCTION

The ability to exchange a given halide in an aryl group for another halide would enormously facilitate the versatility of many transition metal catalyzed cross-coupling reactions.[1−5] For instance, the exchange of less reactive aryl−Cl for aryl−Br or aryl−I bonds would broaden the scope of aryl halide starting materials for many processes now limited to the most reactive aryl-I.[6,7] Only Ni[8,9] and Cu-catalyzed[2,10] aryl halide exchange processes have been reported,[1] whereas Pd-based systems lack precedent. Although no generally successful Pd-catalyzed halide exchange reactions have yet been reported, there has been considerable success in the development of Pd-mediated direct halogenation of aromatic rings,[11−13] and recently a Pd-catalyzed transformation of aryl-triflates to aryl−Cl and aryl−Br has been reported.[14]

Special mention is deserved by the halide exchange reactions that aim to insert a fluorine atom at an aryl group.[15−17] Fluorine forms the strongest single bond to carbon; the combination of its high electronegativity and small size give rise to the unusual properties associated with fluorinated organic compounds, that is, chemical inertness, high thermal stability and high solubility. At present, up to 30−40% of agrochemicals and 20−30% of pharmaceuticals contain at least one fluorine atom, which is usually located at an arene. In light of the importance of fluorinated arenes and the practical limitations of current methods for their preparation,[18−22] the metal-catalyzed conversion of a nonactivated aryl halide with a nucleophilic fluorine source (i.e., an alkali metal fluoride) to yield the corresponding aryl fluoride is a highly sought and desirable transformation.

Transition-metal catalyzed aryl−X fluorination can be envisioned via a three-step catalytic cycle that would involve aryl−X oxidative addition, followed by X- to F-exchange, and finally aryl−F reductive elimination (Scheme 1).[23]

Currently, among all transition metals in any oxidation state, only two Pd-based compounds have been identified as capable of affording C−F bond formation via reductive elimination: Ritter's pyridyl-sulfonamide Pd^{IV} fluoride,[24,25] and Buchwald's phosphine Pd^{II} fluoride.[26] The former was the first example of an aryl−F reductive elimination from a well-defined aryl−Pd^{IV}−F species. On the contrary, Buchwald's compound overcomes the usual reluctance of aryl−Pd^{II}−F species to undergo reductive elimination by using a bulky monodentated phosphine ligand, which stabilizes a 14-electron tricoordinated aryl−Pd^{II}−F species. The latter undergoes aryl-F reductive elimination using aryl triflates or bromides and AgF as reactants in 57−85% yield by thermolysis at ∼100 °C.[26] Buchwald's system stands as the unique example in the literature that follows the largely sought catalytic cycle depicted in Scheme 1. On the contrary, electrophilic fluorinating methodologies ("F^{+}" reagents)[25,27−31] cannot be used for the displacement of X^{-} in nonactivated ArX by F^{-}.[32] Moreover, a Pd^{II}/Pd^{IV} catalytic cycle can be considered as unlikely since intramolecular aryl-X oxidative addition at Pd^{II} finds a single precedent in the literature,[33] and no example of the corresponding intermolecular reaction is known. Ideally, catalytic nucleophilic aryl fluorination should be a mild (room temperature)

Received: June 23, 2011
Published: October 25, 2011

dx.doi.org/10.1021/ja2058567 | J. Am. Chem. Soc. 2011, 133, 19386–19392

Scheme 1. Transition-Metal Catalyzed Aryl−X Fluorination

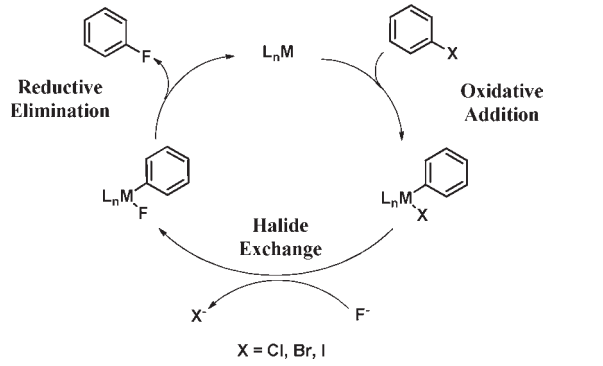

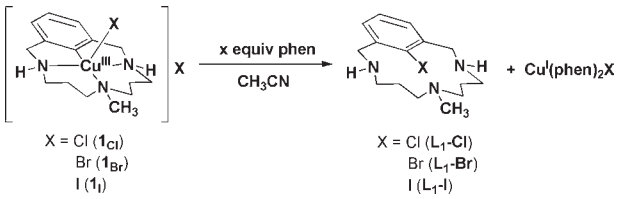

Figure 1. Aryl−X reductive elimination promoted by the addition of 1,10-phenathroline to $\mathbf{1_X}$ complexes at room temperature.

and rapid process to meet the requirements for late-stage aromatic fluorination as well as for the preparation of short-lived ^{18}F-radiolabeled molecular probes for positron emission tomography (PET).[34−36]

We have recently described the reductive elimination of aryl−X from well-defined aryl−Cu^{III}−X complexes (X = Cl, Br, I; Figure 1).[37,38] On the basis of these precedents, herein we report a metal-catalyzed halide exchange from given aryl−X (X = Cl, Br, I) model substrates to heavier or lighter halogenated aryl moieties aryl−Y (Y = F, Cl, Br, I) in an effective manner under mild conditions. Furthermore, we show the direct conversion of aryl chlorides, bromides, and iodides into the corresponding aryl fluorides, using very mild conditions and simple fluoride sources such as AgF and KF, under the catalytic cycle depicted in Scheme 1.

RESULTS AND DISCUSSION

Aryl−X Reductive Elimination in Aryl−Cu^{III}−X Species. In our previous reports on aryl−Cu^{III}−X species $\mathbf{1_X}$ (X = Cl, Br, I, Figure 1), we found that thermolysis was not effective to afford the aryl-X reductive elimination products. Instead, acid addition triggered the reaction at room temperature.[37,38] We were intrigued however, in finding a strategy to avoid the use of an acid source to trigger the reaction, and we reasoned that should a reactant-displaced equilibrium between aryl−Cu^{III}−X and corresponding aryl−X···Cu^{I} species exist, chemical trapping of the Cu^{I} species could drive reductive elimination. Given the large affinity of 1,10-phenanthroline (phen) toward Cu^{I} to afford [Cu^{I}(phen)$_2$]$^+$, we studied the reaction of a given aryl−Cu^{III}−X species with different equivalents of phen. Quantitative formation of the aryl−X elimination products ($\mathbf{L_1}$−X) and [Cu^{I}(phen)$_2$]$^+$ species (Figure 1, Supporting Information Table S1) was observed. Reactions were faster for Cl > Br > I, indicating that the strength of the aryl-X bond formed governed the reactivity. For

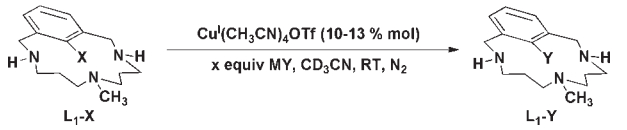

Figure 2. Room temperature halide exchange reactions under catalytic conditions in copper(I).

the slower reactions with $\mathbf{1_I}$, increasing amounts of phen were needed and also minor amounts of side-product **2**, arising from intramolecular aryl-amine reductive elimination, were observed, as documented in previous studies.[39,40] This reactivity demonstrates the existence of a reductive elimination/ oxidative addition Cu^{III}/Cu^{I} equilibrium that opened the door to explore a Cu-catalyzed halide exchange in our $\mathbf{L_1}$−X systems.

Halide Exchange in Aryl−X Model Substrates (X = Cl, Br, I). The conceived catalytic strategy for achieving halide exchange consisted in the addition of a catalytic amount (11 mol %) of a Cu^{I} source ([Cu^{I}(CH$_3$CN)$_4$]OTf, OTf = CF$_3$SO$_3$) together with an excess of the desired halide salt MY (M = Na, Bu$_4$N; Y = Cl, Br, I) (Figure 2). Oxidative addition reactivity of Cu^{I} and aryl−X species in these systems is precedented.[37] Because of that, we expected initial oxidative addition to proceed forming aryl−Cu^{III}−X species. Subsequent halide exchange, and final aryl−Y reductive elimination should furnish aryl−halide exchange products.

As envisioned, aryl−I ($\mathbf{L_1}$−**I**) exchange to afford aryl−Cl ($\mathbf{L_1}$−**Cl**) and aryl−Br ($\mathbf{L_1}$−**Br**) is achieved in nearly quantitative yields at room temperature using acetonitrile as solvent, and Bu$_4$NCl and Bu$_4$NBr, respectively, as halide sources (Table 1, entries 1 and 4).

Spectroscopic monitoring experiments provide strong support that reactions take place via the expected mechanism. In first place, upon addition of Cu^{I} to a solution containing both $\mathbf{L_1}$−**I** and an excess of Bu$_4$NBr or Bu$_4$NCl, an immediate change of color was evident, and was indicative of halide exchange at the Cu^{III} center, resulting in the formation of $\mathbf{1_{Br}}$ or $\mathbf{1_{Cl}}$, respectively. Gradual fading of the solution color indicated the ongoing aryl−Y reductive elimination, as proved by direct ^{1}H NMR and ESI-MS analyses of the final crude mixture. The latter observations agree with a proposal involving aryl−Cu^{III}−Y species as resting state, and the aryl−Y reductive elimination as the rate-limiting step. Indeed, the exchange of I to Br using Bu$_4$NBr salt afforded the $\mathbf{L_1}$−**Br** product in a 87% yield (Table 1, entry 4). A 13 mol % content of the aryl−Cu^{III}−Br ($\mathbf{1_{Br}}$) resting state remained in the final crude mixture (determined by ^{1}H NMR) and accounted for the mass balance of the macrocyclic ligand.

The exchange of aryl−Br and aryl−Cl toward the more reactive aryl−I species could also be accomplished by taking advantage of the poor solubility of NaX (X = Cl, Br) salts in acetonitrile. Catalytic halide exchange from $\mathbf{L_1}$−**Br** to $\mathbf{L_1}$−**I** was achieved in good yields by using 12 mol % of Cu^{I} salt and an excess of soluble NaI in CH$_3$CN at room temperature (Table 1, entries 5−6). In this case, yields reach a top limit of 84% because the final reaction mixture contains a 12% mol content of the corresponding aryl−Cu^{III}−I species ($\mathbf{1_I}$). Nevertheless, halide exchange is clean since only $\mathbf{L_1}$−**I** product and a small quantity of remaining starting material ($\mathbf{L_1}$−**Br**, <5%) are found by ^{1}H NMR in the final reaction mixture after reaction optimization (Table 1, entry 6).

Catalytic halide exchange from $\mathbf{L_1}$−**Cl** to $\mathbf{L_1}$−**I** is extremely slow at room temperature and after 96 h only a 36% yield of the

dx.doi.org/10.1021/ja2058567 |J. Am. Chem. Soc. 2011, 133, 19386–19392

Table 1. Catalytic Halide Exchange Reactions through Aryl−Cu^{III}−Halide Complexes with MY in CD_3CN under N_2 ($[Cu^I(CH_3CN)_4]OTf$ as Cu^I Source)

entry	L_1−X	halide salt (MY)	equiv	time (h)	T (°C)	% yield L_1−Y[a,b]	% starting material
1	L_1−I	Bu_4NCl	5[c]	1.5	25	96	0
2		Bu_4NCl	10[c]	1.5	25	99	0
3		Bu_4NCl	10[d]	1.5	25	0	100
4		Bu_4NBr	10[e]	40	25	87	0
5	L_1−Br	NaI	10[f]	36	25	77	12
6		NaI	20[g]	36	25	84	4
7		Bu_4NCl	10[h]	2	25	99	0
8	L_1−Cl	NaI	10[i]	96	25	36	53
9		NaI	10[j]	24	40	9	91
10		NaI	10[k]	24	40	56 (17)	15
11		NaI	10[l]	24	40	57(2)	31
12		NaI	10[l]	24	50	62(4)	21
13		LiI	10[m]	24	40	5	84
14		Bu_4NI	10[m]	24	40	0 (11)	78
15		NaBr	10[n]	24	25	37	52
16		NaBr	10[n]	24	40	38(10)	39
17		Bu_4NBr	10[i]	24	25	0	89

[a] ^1H NMR yield using trimethoxybenzene as internal standard in CD_3CN. [b] Intramolecular C−N reductive elimination product **2** yield appears in parentheses for some entries. [c] Conditions: $[L_1-I]$ = 9 mM, $[Cu^I]$ = 1 mM (11 mol %). [d] Conditions: $[L_1-I]$ = 9 mM, no addition of copper(I) salt. [e] Conditions: $[L_1-I]$ = 7.6 mM, $[Cu^I]$ = 1 mM (13 mol %). [f] Conditions: $[L_1-Br]$ = 8.6 mM, $[Cu^I]$ = 1 mM (11 mol %). [g] Conditions: $[L_1-Br]$ = 7.6 mM, $[Cu^I]$ = 0.9 mM (12 mol %). [h] Conditions: $[L_1-Br]$ = 9 mM, $[Cu^I]$ = 1 mM (11 mol %). [i] Conditions: $[L_1-Cl]$ = 8.5 mM, $[Cu^I]$ = 0.9 mM (11 mol %). [j] Conditions: $[L_1-Cl]$ = 8.5 mM, no addition of copper(I) salt. [k] Conditions: $[L_1-Cl]$ = 8.5 mM, $[Cu^I]$ = 1 mM (12 mol %). [l] Conditions: $[L_1-Cl]$ = 9 mM, $[Cu^I]$ = 1 mM (11 mol %), acetone-d_6 as solvent. [m] Conditions: $[L_1-Cl]$ = 9 mM, $[Cu^I]$ = 1 mM (11 mol %). [n] Conditions: $[L_1-Cl]$ = 9 mM, $[Cu^I]$ = 0.9 mM (10 mol %).

desired product is obtained using 11 mol % of Cu^I salt and an excess of soluble NaI in CH_3CN (Table 1, entry 8). The reaction performed at 40 °C (Table 1, entry 10) afforded the L_1−I product in moderate yield (56% yield). However, at this temperature, a competing intramolecular side-reaction involving aryl−amine coupling occurs, affording also a 17% of product **2**. The change of CD_3CN solvent by acetone-d_6 affords L_1−I in similar yield (57%) but the contribution of the side reaction is reduced, and **2** is obtained in only 2% yield (Table 1, entry 11).

On the basis of the previous observations, it can be concluded that catalytic halide exchange for a given model aryl−X substrate can be performed by exchanging both toward heavier and also lighter halides. Copper-catalyzed halide exchange reactions are favored toward the product with the strongest C−X bond (C−Cl > C−Br > C−I) when both halide salts (MY and MX) are soluble in the reaction mixture. In this case, transformation from L_1−I and L_1−Br toward lighter aryl halides is obtained rapidly and in high yields. On the other hand, the precipitation of the sodium salts out of the CH_3CN solution (Table 1, entries 8−12, 15−17) is key to understand the catalytic cycle turnover toward heavier halide products. In line with this, no halide exchange is observed by using Bu_4NBr or Bu_4NI as reactants (Table 1, entries 14 and 17, respectively). This reactivity resembles a previously reported Cu-catalyzed aromatic Finkelstein reactivity, where aryl−Br subzstrates were converted to aryl−I products.[2]

A general mechanistic proposal for these catalytic halide exchange reactions taking place at our systems is depicted in Figure 3. In all cases, the resting state is the aryl−Cu^{III}−Y species, where Y is the halide (in excess) being inserted. Several parameters influence the catalytic cycle but most predominantly, the strength of the aryl−X bond and the low solubility of the MX salt (X being

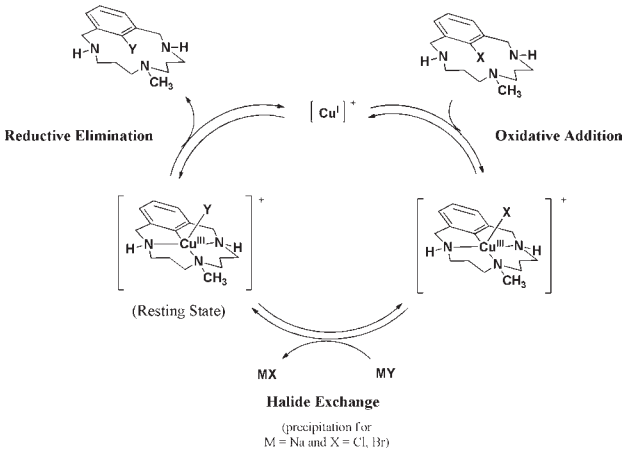

Figure 3. Mechanism of copper(I)-catalyzed halide exchange reactions through aryl−Cu^{III}−X complexes as intermediates (X = I, Br, Cl).

the removed halide) are key to overcome the reversibility of the aryl−X oxidative addition step.

Fluoride Insertion To Obtain Aryl−F Products. Since catalytic halide exchange mediated by a Cu^I/Cu^{III} cycle was proven to be efficient with the combination of any pair of aryl−X and MY (where X, Y = Cl, Br, I) reagents, we were intrigued by the possibility to exchange a given aryl−X by fluoride following the same catalytic cycle (Figure 3 and Scheme 1). We first studied the stoichiometric reaction of complex aryl−Cu^{III}−Cl ($\mathbf{1}_{Cl}$) with AgF and KF as sources of fluoride anions (Figure 4, Table 2). The reaction was performed in CH_3CN at room temperature, and final reaction mixtures were characterized by ^1H NMR and ESI-MS.

To our delight, after reaction optimization, the spectroscopic analyses provide unequivocal evidence for the formation of aryl−F product ($\mathbf{L_1}$−**F**) (C−F bond detected by ^{19}F-NMR at −122.5 ppm in DMSO-d_6) in up to 91% yield after reaction optimization.

Catalytic fluoride exchange insertion at $\mathbf{L_1}$−**X** (X = Cl, Br, I) turned out to be a more problematic transformation. Silver fluoride was initially chosen since it gave the best results for stoichiometric reactions. Direct addition of 2 equiv of AgF in CH_3CN to a solution of $\mathbf{L_1}$−**Cl** and 10 mol % of $[Cu^I(CH_3CN)_4]OTf$ gave $\mathbf{L_1}$−**F** product in low yield (40%). That is presumably due to decomposition of the aryl−Cu^{III}−Cl initially formed under the very basic reaction conditions. To address this problem, the experimental procedure was modified by adding the AgF solution in a slow dropwise manner. Under these conditions, reaction proceeded to full conversion of $\mathbf{L_1}$−**Cl** to a 76% yield of $\mathbf{L_1}$−**F**, along with a 20% yield of the intramolecular aryl−amine coupling side-product **2** (Figure 5, Table 3). Similar results were obtained by using $\mathbf{L_1}$−**Br** as reactant, affording $\mathbf{L_1}$−**F** in 71% yield. On the contrary, other fluoride sources (Bu_4NF, Me_4NF or CsF) proved to be completely inefficient.

The high basicity of F^- is well-documented,[15,16,41] and we suspected that the secondary amines in aryl−Cu^{III}−X may be keen to deprotonation.[42] To avoid that, permethylated macrocyclic $\mathbf{L_5}$−**X** substrates (X = Cl, Br), which are structurally related to $\mathbf{L_1}$−**Cl** and $\mathbf{L_1}$−**Br**, respectively, were prepared and studied in the fluoride insertion catalysis. Most rewarding, a quantitative formation of aryl−F product, that is, $\mathbf{L_5}$−**F** (Figure 5, Table 3), was accomplished with these systems.

The reactivity of the systems based in permethylated macrocyclic $\mathbf{L_5}$−**X** substrates (X = Cl, Br) exhibits significant differences with regard to $\mathbf{L_1}$−**X** analogues. On one hand, dropwise addition of the fluoride source was not required for the former, which suggested that the strong basicity of the fluoride anion directly affected the secondary amines in the reactions that use $\mathbf{L_1}$−**X**. On the other hand, fluoride insertion at $\mathbf{L_5}$−**X** substrates (X = Cl, Br) failed when reactions were performed in CH_3CN. We reasoned that this may be due to the well-established overenhanced stability of Cu^I species with ligands bearing tertiary amines in acetonitrile.[43,44] Because of that, a mixture of acetone and CH_3CN was used instead. To our delight, in this solvent mixture fluoride insertion in $\mathbf{L_1}$−**Cl** and $\mathbf{L_1}$−**Br** was basically quantitative (>97% yield; Table 3, entries 4 and 7). Nonetheless, the content of Cu^I catalyst could be reduced to 5% affording $\mathbf{L_5}$−**F** in excellent yield, although extending the reaction time (Table 3, entry 5).

Fluoride exchange reactions leading to $\mathbf{L_1}$−**F** and $\mathbf{L_5}$−**F** can be also accommodated by invoking the mechanistic proposal involving a Cu^I/Cu^{III} catalytic cycle. Aryl−X oxidative addition at Cu^I (Scheme 1, step 1) to form aryl−Cu^{III}−X species is well-known within these systems.[37] The subsequent X^- to F^- exchange to form a putative aryl−Cu^{III}−F (Scheme 1, step 2) is not detected experimentally, and only the final aryl−F product is obtained. The latter observation suggests a rate-limiting halide to fluoride exchange followed by a fast reductive elimination step from an aryl−Cu^{III}−F species (Scheme 1, step 3). Consistent with this scenario, ^{1}H NMR monitoring of the reaction of $\mathbf{1_{Br}}$ with AgF to form $\mathbf{L_1}$−**F** shows the disappearance of $\mathbf{1_{Br}}$ signals to afford the new $\mathbf{L_1}$−**F** compound at room temperature, without the presence of any other intermediate species (Figure S3).

Effect of Water Content on Halide Exchange Catalysis. Given the highly hygroscopic character of the halide salts used in the halide exchange catalysis, we studied the role of water in three representative halide exchange reactions by performing the reactions under strict anhydrous conditions and adding 10, 50, or 100 equiv of H_2O. The copper-catalyzed halide exchange from $\mathbf{L_1}$−**I** to $\mathbf{L_1}$−**Cl** using Bu_4NCl as the halide salt is not affected by the presence of water (0−100 equiv of H_2O) (see Table 1, entry 2, and Supporting Information Table S2). In the reverse reaction from $\mathbf{L_1}$−**Cl** to $\mathbf{L_1}$−**I** using 10 equiv of NaI, the reaction is also not affected by small amounts of water (10 equiv), but yields decrease when larger amounts are added (50−100 equiv) (see Table 1, entry 10, and Supporting Information Table S2). The latter results can be rationalized by the improved solubility of

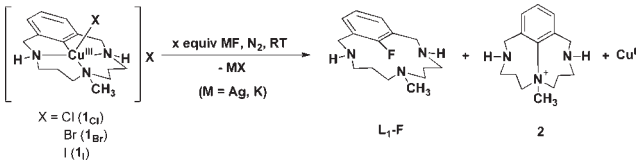

Figure 4. Room temperature nucleophilic fluorination of $\mathbf{1_X}$ with MF salts (M = Ag, K) to afford $\mathbf{L_1}$−**F** and Cu^I (compound **2** is also obtained in minor quantities).

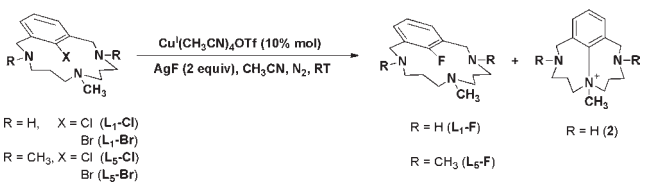

Figure 5. Catalytic fluorination of aryl−X (X = Cl, Br) substrates at room temperature.

Table 2. Stoichiometric C−F Bond Formation through Aryl−Cu^{III}−X Complexes with Several Equivalents of MF (M = Ag, K) at 298 K in CH_3CN under N_2

entry	complex	MF (equiv)	solvent	time (h)	$\mathbf{L_1}$−**F** % yield[a]	**2** % yield
1	$\mathbf{1_{Cl}}$	AgF (5)	CH_3CN	8	74	23
2		AgF (8)	CH_3CN	8	91	8
3		AgF (12)	CH_3CN	8	77	22
4		KF (5)[c]	CH_3CN/DMSO-d_6 (8:1)	24	31	36
5	$\mathbf{1_{Br}}$	AgF (5)	CH_3CN	4	84	14
6		AgF (5)[b]	CH_3CN	1	74	24
7		KF (5)[c]	CH_3CN/DMSO-d_6 (8:1)	100	23	47
8	$\mathbf{1_I}$	AgF (5)	CH_3CN	3	76	22

[a] NMR yields using 1,3,5-trimethoxybenzene as an internal standard in DMSO-d_6 after extractions of copper with $NH_4OH/MgSO_4$. [b] Reaction performed at 45 °C. [c] Reactions with KF also afforded a 33% (entry 4) and 27% (entry 7) yield of L_1−H product.

dx.doi.org/10.1021/ja2058567 |J. Am. Chem. Soc. 2011, 133, 19386–19392

Table 3. Cu^{I}-Catalyzed C−F Bond Formation through the Reaction of L_1−X (X = Cl, Br) Substrates with 2 equiv of AgF at 298 K (CH_3CN, under N_2, Light Excluded)

entry	L_1−X	% mol Cu^{I} [a]	solvent	time (h)	L_x−F % yield[b]	2 % yield
1	L_1−Cl	10	CH_3CN	6	76[c]	20
2		0	CH_3CN	6	0	0
3	L_1−Br	10	CH_3CN	4	71[c]	21
4	L_5−Cl	10	CH_3CN/acetone (1:3)	12	98	0
5		5	CH_3CN/acetone (1:3)	24	98	
6		0	CH_3CN/acetone (1:3)	24	0	
7	L_5−Br	10	CH_3CN: acetone (1:3)	24	97	

[a] As $[Cu^{I}(CH_3CN)_4]OTf$. [b] NMR yields using 1,3,5-trimethoxybenzene as an internal standard in DMSO-d_6 after extractions of copper with NH_4OH/$MgSO_4$. [c] Reactions also afforded a 4% (entry 1) and 8% (entry 3) yield of another nonidentified product.

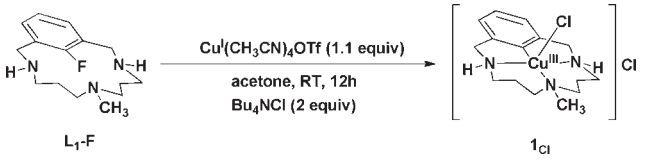

Figure 6. Defluorination of L_1−F mediated by Cu^{I} at room temperature to afford $\mathbf{1}_{Cl}$.

NaCl formed upon water addition. Efficient NaCl precipitation is crucial in order to drive the reaction toward the product with a weaker C−X bond. An improved solubility thus reduces the reaction yields. On the contrary, when the Ar−Y bond strength to be formed is higher that the Ar−X bond broken (i.e., exchange from L_1−I to L_1−Cl), the effect of water is not significant.

To address possible effects of water in the fluorination reactions, we have studied the catalytic fluorination of L_1−Cl under strictly anhydrous conditions, and also by adding 10 and 50 equiv of H_2O (see Table 3, entry 1, and Supporting Information Table S2). The yields of fluorinated product L_1−F show a progressive decrease as the number of H_2O equivalents added increase (from 75% yield for 0 equiv of H_2O added down to 32% L_1−F if 50 equiv of H_2O are added). Indeed, reactions progress more slowly and the presence of water triggers a side-reaction that produces minor amounts of L_1−H product (<10%). Clearly, strictly anhydrous conditions are required to obtain the best yields of fluorination for these systems.[45]

Defluorination of Aryl−F to Aryl−Cl. At this point, we speculated about the possibility of going a step further and wondered if aryl−F substrates could be activated by Cu^{I}, and undergo further halide exchange. The combination of equimolar amounts of Cu^{I} and L_1−F in CH_3CN, with the subsequent addition of excess Bu_4NCl, did not afford any fluoride exchange. However, by changing the solvent to acetone, the same reactants afforded the formation of a red colored solution, corresponding to the formation of aryl−Cu^{III}−Cl ($\mathbf{1}_{Cl}$) (Figure 6) in 75% yield (estimated by ^1H NMR, see Supporting Information Figure S7). Reaction of $\mathbf{1}_{Cl}$ with phen affords L_1−Cl quantitatively (Figure 1). The most plausible explanation for this result is that the energy barrier corresponding to the aryl−F oxidative addition step to afford aryl−Cu^{III}−F is lowered, and rapid formation of aryl−Cu^{III}−Cl ($\mathbf{1}_{Cl}$) upon addition of excess Cl^- is achieved. The low solubility of the latter in acetone displaces all equilibria toward its formation. To the best of our knowledge, this is the first example of aromatic defluorination using a Group 11 metal, since the field is vastly dominated by reactions mediated by Group 9 and 10 transition metals.[17,46]

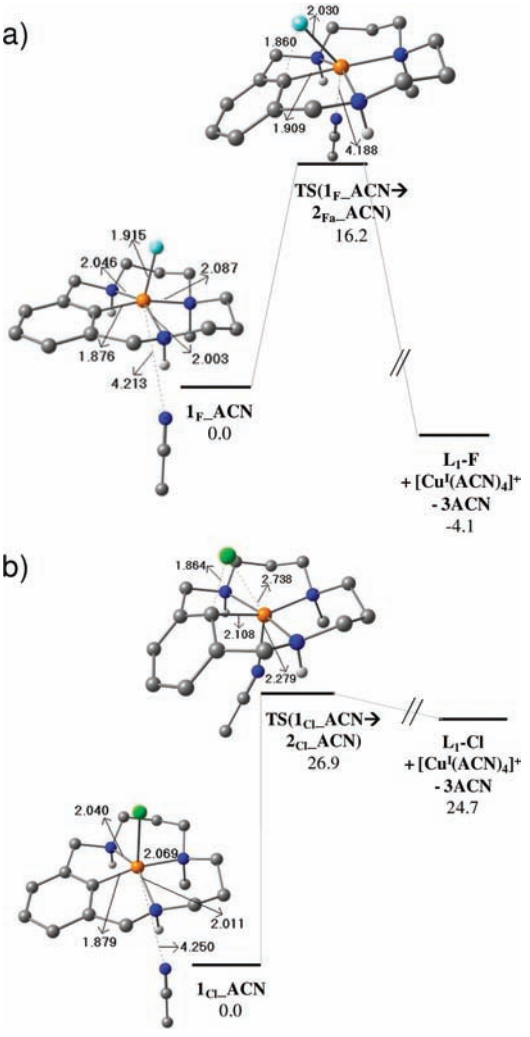

Figure 7. DFT studies of (a) the L_1−F reductive elimination reaction from aryl−Cu^{III}−F, and (b) the L_1−Cl reductive elimination from aryl−Cu^{III}−Cl ($\mathbf{1}_{Cl}$). Relative Gibbs energy values in acetonitrile solution are given in kcal mol^{-1} and selected bond distances in Å (one explicit CH_3CN molecule (ACN) has been considered in the calculations; H atoms are omitted for clarity except for N−H moieties; see full calculated reaction pathways in Supporting Information Figure S33).

Computational Studies. DFT computational studies were performed with the aim of providing a theoretical basis to support the proposed mechanistic scheme, with special attention to the C−F bond forming-cleavage reaction.[47] This analysis was directed at addressing the following specific aspects: (a) the feasibility and molecular structure of the putative aryl−Cu^{III}−F species; (b) the energetics and viability of the aryl−F reductive elimination from aryl−Cu^{III}−F species; and (c) the energetic viability of the oxidative addition/reductive elimination connecting "aryl-Cl + Cu^{I}", and aryl−Cu^{III}−Cl species, as well as the effect of acetonitrile in these transformations.

(a) The computed molecular structure of aryl−Cu^{III}−F species (**1_{F}_ACN**) resembles that of the previously crystallographically characterized aryl−Cu^{III}−X family of species (Figure 7a).[37] The copper ion adopts a distorted square pyramidal geometry, and the fluoride anion occupies the axial position, with a Cu−F distance of 1.915 Å (distance similar to an axial Pd^{IV}−F bond reported in the literature[24]). The aryl ligand occupies one of the equatorial positions and it is in a *cis*-relative position with respect to the F^{-}. An acetonitrile molecule has a weak interaction ($d_{Cu\text{-}ACN}$ = 4.213 Å) in the empty axial coordination site of the copper ion.

(b) **L_1−F** reductive elimination from **1_{F}_ACN** involves the formation of the aryl−F bond and the formal $2e^{-}$ reduction of the Cu^{III} center to Cu^{I} (step 3 in Scheme 1) to afford the **L_1−F**···Cu^{I} product. The corresponding transition state (TS) was found with a small energy barrier ($\Delta G^{\ddagger}$ = 16.2 kcal mol^{-1}), whereas the **L_1−F**···Cu^{I} product was stabilized to a relative Gibbs energy of −4.1 kcal mol^{-1} with respect to the aryl−Cu^{III}−F species (**1_{F}_ACN**) (Figure 7a). The latter values are in agreement with a fast and irreversible aryl−F reductive elimination step.

(c) Aryl−Cl reductive elimination from **1_{Cl}_ACN** was also studied computationally (Figure 7b), and a much higher barrier for the aryl−Cl reductive elimination step ($\Delta G^{\ddagger}$ = 26.9 kcal mol^{-1}) was found. Furthermore, the **L_1−Cl**···Cu^{I} product remains at 24.7 kcal mol^{-1} (Figure 7b). That clearly indicates the ease of the downhill reversal oxidative addition reaction between Cu^{I} and **L_1−Cl**, as already observed experimentally.[37]

Overall, computational studies reveal that aryl−F reductive elimination is a much more favored process than aryl−Cl reductive elimination, which is in agreement with the experimental observations and explained by the strength of the aryl−F bond being formed.

Concluding Remarks. In conclusion, we present here the first transition-metal-based system capable of catalyzing halide exchange reactions in all directions along Group 17 of the Periodic Table, including aryl fluorination and defluorination. Reactions occur under mild, room temperature conditions. The halide-exchange reactions occur through a Cu^{I}/Cu^{III} redox catalytic cycle, thus providing proof-of-concept of the ability of copper to enable such transformations. We propose that the stabilization of aryl−Cu^{III} intermediate species is at the basis of this rather unique reactivity, because in this case activation barriers corresponding to the Cu^{I}/Cu^{III} couple are small, and the Cu^{III} oxidation state becomes thermodynamically enabled. This work provides fundamental mechanistic understanding that may help in the design of efficient Cu-catalysts for halide exchange in simple aryl halide substrates. Moreover, quantitative nucleophilic fluorination of aryl−X model substrates catalyzed by Cu^{I} via aryl−F reductive elimination has been proven for the first time with a metal different than Pd, following a Cu^{I}/Cu^{III} catalytic cycle and under room temperature conditions. Although the present work relies on a highly elaborated system, we believe these results might provide inspiration to develop Cu-based fluorinating technologies with synthetic utility on the basis of mechanistic understanding.

■ ASSOCIATED CONTENT

Supporting Information. Chemical compound full characterization; complete description of computational details; full calculated reaction pathways; XYZ coordinates for all DFT calculated molecules. This material is available free of charge via the Internet at http://pubs.acs.org.

■ AUTHOR INFORMATION

Corresponding Author
xavi.ribas@udg.edu

■ ACKNOWLEDGMENT

We thank Prof. S. S. Stahl (Univ. of Wisconsin, Madison, WI) for fruitful comments and for early experiments conducted by A.C. in Stahl's lab. We acknowledge financial support from MICINN of Spain (CTQ2009-08464/BQU to M.C., CTQ2008-03077/BQU and CTQ2011-23156/BQU to M.S., Consolider-Ingenio CSD2010-00065, and Ph.D. grant to A.C.), European Research Council for Project ERC-2011-StG-277801 and the Catalan DIUE of the Generalitat de Catalunya (2009SGR637 to M.S., and a Ph.D. grant to M. Canta). X.R., M.C., and M.S. thank ICREA-Academia awards. We thank STR's from UdG for technical support, and we also acknowledge the Centre de Serveis Científics i Acadèmics de Catalunya (CESCA) for partial funding of computer time.

■ REFERENCES

(1) Sheppard, T. D. *Org. Biomol. Chem.* **2009**, *7*, 1043–1052.
(2) Klapars, A.; Buchwald, S. L. *J. Am. Chem. Soc.* **2002**, *124*, 14844–14845.
(3) Roy, A. H.; Hartwig, J. F. *J. Am. Chem. Soc.* **2003**, *125*, 13944–13945.
(4) Vigalok, A. *Chem.—Eur. J.* **2008**, *14*, 5102–5108.
(5) Vigalok, A.; Kaspi, A. W. *Top. Organomet. Chem.* **2010**, *31*, 19–38.
(6) Surry, D. S.; Buchwald, S. L. *Chem. Sci.* **2010**, *1*, 13–31.
(7) Larsson, P.-F.; Correa, A.; Carril, M.; Norrby, P.-O.; Bolm, C. *Angew. Chem., Int. Ed.* **2009**, *48*, 5691–5693.
(8) Cramer, R.; Coulson, D. R. *J. Org. Chem.* **1975**, *40*, 2267–2273.
(9) Arvela, R. K.; Leadbeater, N. E. *Synlett* **2003**, 1145–1148.
(10) Couture, C.; Paine, A. J. *Can. J. Chem.* **1985**, *63*, 111–120.
(11) Kalyani, D.; Dick, A. R.; Anani, W. Q.; Sanford, M. S. *Org. Lett.* **2006**, *8*, 2523–2526.
(12) Chen, X.; Hao, X.-S.; Goodhue, C. E.; Yu, J.-Q. *J. Am. Chem. Soc.* **2006**, *128*, 6790–6791.
(13) Mei, T.-S.; Giri, R.; Maugel, N.; Yu, J.-Q. *Angew. Chem., Int. Ed.* **2008**, *47*, 5215–5219.
(14) Shen, X.; Hyde, A. M.; Buchwald, S. L. *J. Am. Chem. Soc.* **2010**, *132*, 14076–14078.
(15) Furuya, T.; Kamlet, A. S.; Ritter, T. *Nature* **2011**, *473*, 470–477.
(16) Grushin, V. V. *Acc. Chem. Res.* **2010**, *43*, 160–171.
(17) Torrens, H. *Coord. Chem. Rev.* **2005**, *249*, 1957–1985.
(18) Balz, G.; Schiemann, G. *Ber. Dtsch. Chem. Ges.* **1927**, *60*, 1186–1190.
(19) Miller, J. In *Aromatic Nucleophilic Substitution*; Elsevier: London, 1968.

(20) Finger, G. C.; Kruse, C. W. *J. Am. Chem. Soc.* **1956**, *78*, 6034–6037.
(21) Langlois, B.; Gilbert, L.; Forat, G. *Ind. Chem. Libr.* **1996**, *8*, 244–292.
(22) Grushin, V. V., U.S. Patent 7,202,388, 2007.
(23) Grushin, V. V. *Chem.—Eur. J.* **2002**, *8*, 1006–1014.
(24) Furuya, T.; Ritter, T. *J. Am. Chem. Soc.* **2008**, *130*, 10060–10061.
(25) Furuya, T.; Benitez, D.; Tkatchouk, E.; Strom, A. E.; Tang, P.; Goddard, W. A., III; Ritter, T. *J. Am. Chem. Soc.* **2010**, *132*, 3793–3807.
(26) Watson, D. A.; Su, M.; Teverovskiy, G.; Zhang, Y.; García-Fortanet, J.; Kinzel, T.; Buchwald, S. L. *Science* **2009**, *325*, 1661–1664.
(27) Hull, K. L.; Anani, W. Q.; Sanford, M. S. *J. Am. Chem. Soc.* **2006**, *128*, 7134–7135.
(28) Ball, N. D.; Sanford, M. S. *J. Am. Chem. Soc.* **2009**, *131*, 3796–3797.
(29) Wang, X.; Mei, T.-S.; Yu, J.-Q. *J. Am. Chem. Soc.* **2009**, *131*, 7520–7521.
(30) Brown, J. M.; Gouverneur, V. *Angew. Chem., Int. Ed.* **2009**, *48*, 8610–8614.
(31) Chan, K. S. L.; Wasa, M.; Wang, X.; Yu, J.-Q. *Angew. Chem., Int. Ed.* **2011**, *50*, 9081–9084.
(32) Grushin, V. V.; Marshall, W. J. *Organometallics* **2008**, *27*, 4825–4828.
(33) Vicente, J.; Arcas, A.; Juliá-Hernández, F.; Bautista, D. *Angew. Chem., Int. Ed.* **2011**, *50*, 6896–6899.
(34) Miller, P. W.; Long, N. J.; Vilar, R.; Gee, A. D. *Angew Chem., Int. Ed.* **2008**, *47*, 8998–9033.
(35) Li, L.; Hopkinson, M. N.; Yona, R. L.; Bejot, R.; Gee, A. D.; Gouverneur, V. *Chem. Sci.* **2011**, *2*, 123–131.
(36) Cai, L.; Lu, S.; Pike, V. W. *Eur. J. Org. Chem.* **2008**, 2853–2873.
(37) Casitas, A.; King, A. E.; Parella, T.; Costas, M.; Stahl, S. S.; Ribas, X. *Chem. Sci.* **2010**, *1*, 326–330.
(38) Casitas, A.; Poater, A.; Solà, M.; Stahl, S. S.; Costas, M.; Ribas, X. *Dalton Trans.* **2010**, *39*, 10458–10463.
(39) Huffman, L. M.; Stahl, S. S. *J. Am. Chem. Soc.* **2008**, *130*, 9196–9197.
(40) Huffman, L. M.; Stahl, S. S. *Dalton Trans.* **2011**, *40*, 8959–8963.
(41) Grushin, V. V. *Angew. Chem., Int. Ed.* **1998**, *37*, 994–996.
(42) Casitas, A.; Ioannidis, N.; Mitrikas, G.; Costas, M.; Ribas, X. *Dalton Trans.* **2011**, *40*, 8796–8799.
(43) Xifra, R.; Ribas, X.; Llobet, A.; Poater, A.; Duran, M.; Solà, M.; Stack, T. D. P.; Benet-Buchholz, J.; Donnadieu, B.; Mahía, J.; Parella, T. *Chem.—Eur. J.* **2005**, *11*, 5146–5156.
(44) Ribas, X.; Xifra, R.; Parella, T.; Poater, A.; Solà, M.; Llobet, A. *Angew. Chem., Int. Ed.* **2006**, *45*, 2941–2944.
(45) We thank a reviewer for encouraging us to conduct the study of the role of water in our halide exchange catalysis.
(46) Sun, A. D.; Love, J. A. *Dalton Trans.* **2010**, *39*, 10362–10374.
(47) The B3LYP/6-31G(d) method has been used. See Supporting Information for further details on the computational methodology.

■ NOTE ADDED IN PROOF

A [18F] fluoride-derived electrophilic fluorination strategy for PET imaging has been reported during proof correction: Lee, E.; Kamlet, A. S.; Powers, D. C.; Neumann, C. N.; Boursalian, G. B.; Furuya, T.; Choi, D. C.; Hooker, J. M.; Ritter, T. *Science* **2011**, *334*, 639-642.